THE JOURNAL OF PHYSICAL CHEMISTRY LETTERS
A JOURNAL OF THE AMERICAN CHEMICAL SOCIETY

pubs.acs.org/JPCL

Letter

Ionization Pathway Interference in Photoionization Time Delays in Molecules

Deep Mukherjee,* Upendra Harbola,* and Shaul Mukamel

Cite This: *J. Phys. Chem. Lett.* 2024, 15, 3866−3870

Read Online

ACCESS | Metrics & More | Article Recommendations | Supporting Information

ABSTRACT: The photoionization time-delay in linear conjugated molecules is computed using the Wigner scattering approach. We find that, in general, there are two additive contributions to the ionization time-delays. One originates from interferences between various ionization pathways that belong to different cationic eigenstates, while the other is due to time delays associated with each pathway and originates due to electron−electron correlations in the molecule. The former contribution scales up rapidly with the conjugation length, leading to larger time delays, as observed in recent experiments, while the latter is much less sensitive to the molecular conjugation.

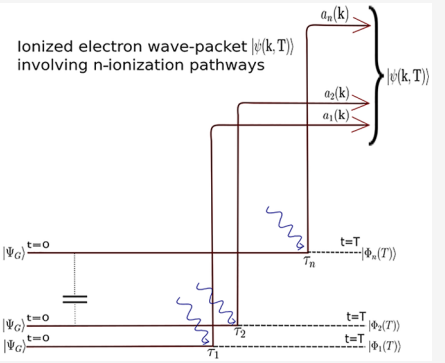

Electron dynamics[1,2] is the fundamental step in all chemical and physical changes in molecules. In this regard, photoionization dynamics[3−6] in molecules has gained a lot of research interest in the last couple of decades. Newly developed ultrashort attosecond *XUV* pulses[7−11] have been used to measure time-scales of electron (hole) dynamics[12−17] and photoionization time delays[18−22] in atoms and molecules. In ref 23, the ionization times of small water clusters were measured using the RABBIT technique,[24,25] and it was shown that the time-scale increases with the cluster size. Similar results were reported for linear-conjugated molecules.[23,26] A recent experimental study[27] has revealed the interference effects in photoionization time delay in Krypton dimer.

In this work, we employ the Huckel model for linear conjugated molecules to compute photoionization time delays. We use the Wigner scattering approach[28] to compute the ionization time delays by visualizing the ionization as a half-scattering (bound to continuum) process. We find that ionization time delay has two contributions: one, that arises as a result of the time delay associated with a given ionization pathway that leaves the cation in a particular eigenstate and originates due to the (many-body) electron correlations, while the other contribution is solely due to interference between various ionization pathways. We further find that the observed increase in the time delay with conjugation is almost entirely due to the interference contribution. The relative weight of each contribution can be controlled by manipulating the ionizing pulse parameters. A spectrally broader pulse offers additional ionization pathways, leading to increased interferences and hence the larger quantum contribution. On the other hand, a simultaneous measurement of the ionized electron energy and the final state of the cation completely removes the interference contribution. Our results provide a new insight into the photoionization time delays in molecules and opens a possibility to manipulate photoionization time delays by controlling the interfering pathways in molecular chains and clusters by varying the pulse parameters or by adjusting the measurement setup.

Consider a molecular system interacting with an attosecond ionizing pulse. The total Hamiltonian is $H(t) = \mathcal{H} - \mu\cdot\mathbf{E}(t)$, where $\mathcal{H}$ is the molecular Hamiltonian and μ is molecule dipole vector interacting with the pulse electric field vector. Note that typically the attosecond pulse peak energy lies in the range 10−100 eV and the dipole approximation remains valid.

The Wigner time delay[28] is identified with the rate of change of the phase of the scattered wave packet with respect to the scattered energy. We compute the ionized electron wavepacket in a scattered state with momentum $\mathbf{k}$. We start from the formal (exact) solution[29] of the time-dependent Schrodinger equation for the Hamiltonian $H(t)$ ($\hbar$= 1),

$$|\Psi(t)\rangle = i\int_0^t \mathrm{d}\tau \mathrm{e}^{-i\int_\tau^t \mathrm{d}t' H(t')}\boldsymbol{\mu}\cdot\mathbf{E}(\tau)\mathrm{e}^{-i\mathcal{H}\tau}|\Psi_G\rangle + \mathrm{e}^{-i\mathcal{H}t}|\Psi_G\rangle \tag{1}$$

where $|\Psi_G\rangle$ is the ground state of the neutral molecule. The state $|\Psi(t)\rangle$ is given by linear combination of the scattered (the

Received: January 15, 2024
Revised: March 28, 2024
Accepted: March 28, 2024
Published: April 1, 2024

first term on the RHS) and the unscattered amplitudes. After ionization, the cation can be in the ground or any of its excited states, $|\Phi_n\rangle$, where $n = 0$ denotes the ground state. For a scattered state $|\Phi_n(\mathbf{k})\rangle$ denoting an electron in free-state $|\mathbf{k}\rangle$ and the cation in state $|\Phi_n\rangle$, the scattered electron amplitude $a_n(\mathbf{k})$ can be obtained by projecting the scattered state onto the total state $|\Psi(t)\rangle$, $a_n(\mathbf{k}) = \langle\Phi_n(\mathbf{k})|\Psi(t)\rangle$,

$$a_n(\mathbf{k}, t) = i\int_0^t \mathrm{d}\tau\langle\Phi_n(\mathbf{k})|\mathrm{e}^{-i\int_\tau^t \mathrm{d}t' H(t')}\boldsymbol{\mu}\cdot\mathbf{E}(\tau)\mathrm{e}^{-i\mathcal{H}\tau}|\Psi_G\rangle \tag{2}$$

Note that $a_n(\mathbf{k})$ represents contribution to the electron wavepacket coming from the ionization pathway where the final state of the cation is $|\Phi_n\rangle$. We denote it as the nth pathway. The ionized electron wavepacket $\psi(\mathbf{k})$ is then obtained by summing the contributions from all pathways (tracing out the information on the cation states), $\psi(\mathbf{k}) = \sum_n |a_n(\mathbf{k})|\mathrm{e}^{i\phi_n(\mathbf{k})}$, where $\phi_n(\mathbf{k})$ is the phase associated with the nth pathway. This allows us to define an ionization time delay $\mathcal{T}_n(\mathbf{k})$ associated with each pathway using the Wigner definition:[28] $\mathcal{T}_n(\mathbf{k}) = \frac{1}{k}\frac{\mathrm{d}\phi_n(\mathbf{k})}{\mathrm{d}k}$, where $k = |\mathbf{k}|$. The net time delay depends on the phase of the total wavepacket $\psi(\mathbf{k})$ and can be expressed as[30] $\mathcal{T}(\mathbf{k}) = \mathcal{T}_C(\mathbf{k}) + \mathcal{T}_Q(\mathbf{k})$, where

$$\mathcal{T}_C(\mathbf{k}) = \frac{\sum_{nm}\mathcal{T}_n(\mathbf{k})\cos(\phi_{nm}(\mathbf{k}))|a_n(\mathbf{k})||a_m(\mathbf{k})|}{\sum_{nm}\cos(\phi_{nm}(\mathbf{k}))|a_n(\mathbf{k})||a_m(\mathbf{k})|}$$

$$\mathcal{T}_Q(\mathbf{k}) = \frac{\sum_{nm}\frac{1}{k}\sin(\phi_{nm}(\mathbf{k}))|a_n(\mathbf{k})|'|a_m(\mathbf{k})|}{\sum_{nm}\cos(\phi_{nm}(\mathbf{k}))|a_n(\mathbf{k})||a_m(\mathbf{k})|} \tag{3}$$

with $\phi_{nm}(\mathbf{k}) = \phi_n(\mathbf{k}) - \phi_m(\mathbf{k})$ and $|a_n(\mathbf{k})|'$ is the derivative of $|a_n(\mathbf{k})|$ with respect to k. Note that $\mathcal{T}_C(\mathbf{k})$ is an average of time delays $\mathcal{T}_n(\mathbf{k})$ associated with individual pathways weighted by the probability $\mathcal{P}_n(\mathbf{k}) = \frac{\sum_m \cos(\phi_{nm}(\mathbf{k}))\,|a_n(\mathbf{k})\,\|\,a_m(\mathbf{k})|}{\sum_{nm}\cos(\phi_{nm}(\mathbf{k}))\,|a_n(\mathbf{k})\,\|\,a_m(\mathbf{k})|}$. On the other hand, $\mathcal{T}_Q(\mathbf{k})$ originates solely due to interference between amplitudes from various pathways.

If all pathways have constant but different phases, $\mathcal{T}_C$ vanishes and the total time delay is entirely due to the interference contribution. As demonstrated below, this is the case when the electron−electron interaction is ignored. On the other hand, if $\phi_n(\mathbf{k}) = \phi_m(\mathbf{k}) \neq$ constant, $\mathcal{T}_Q$ vanishes and only $\mathcal{T}_C$ contributes. Clearly, when the ionized electron momentum $\mathbf{k}$ and the cation state $|\Phi_n\rangle$ are simultaneously measured, only the nth pathway is selected and, as a consequence, $\mathcal{T}_Q = 0$.

A Simple Model: We consider photoionization delays in the valence ionization from pi-conjugated linear molecules. These molecules are potential candidates for applications in optoelectronic devices.[31] It is therefore interesting to study their electron ionization and hole dynamics. Moreover, due to their almost independent sigma- and pi-electron structures, to lowest-order approximation, these molecules can be studied using the Huckel model,[32] which is analytically tractable.

The Hamiltonian for a conjugated molecule with N-atoms can be approximated as (in atomic units)

$$\mathcal{H} = -\frac{1}{2}\sum_{m=1}^{N}\nabla_m^2 - \sum_{m=1}^{N}\sum_{M=0}^{N-1}\frac{q^*}{|\mathbf{r}_m - MR|} + \sum_{mn}\frac{1}{|\mathbf{r}_n - \mathbf{r}_m|} + \gamma(R - R_0)^2 \tag{4}$$

where the first term on the RHS denotes the kinetic energy of the pi-electrons, the second term is the Coulomb interaction between the pi-electrons and the nuclei with each nucleus having an effective charge of q^* due to the screening from sigma-electrons, which are not included explicitly, and R is the distance between two successive atoms. The molecular axis is along the z-axis. We have assumed that the energy of the sigma-structure of the molecule, which includes the kinetic and potential energy of nuclei and all sigma-electrons, is given by a harmonic potential where R changes around some equilibrium distance R_0. This approximation is not crucial as nuclei are supposed to be frozen during the attosecond (10^{-18} s) electronic time scale and the ionization dynamics. We have parametrized the energy corresponding to the sigma-structure mainly to reproduce the ground state energy of the molecule. This is important because the ionized electron is ejected from the neutral ground state having some energy. If this energy is too low, the attosecond pulse may not have sufficient energy to ionize the electron. Thus, to make sure that we remain close to experimentally realizable attoscecond pulses, it is important to have the ground state energy close to the actual one.

In a typical attosecond photoionization experiment, the ionizing pulse is weak and can be treated perturbatively. We assume a Gaussian pulse $E(t) = \mathcal{E}\mathrm{e}^{-\alpha t^2}\cos(\omega_c t)$ and evaluate $a_n(\mathbf{k}, t)$ using the first-order perturbation theory. Furthermore, since the ionized electron is detected much after the attosecond pulse is over, we can replace $t \to \infty$ in eq 2. After some straightforward algebra, we obtain[30]

$$a_n(\mathbf{k}) = i\mathcal{E}e^{-\left(E_G - E_n + \omega_c + \frac{k^2}{2}\right)^2/4\alpha}\langle\Phi_n|\mu_z|\Psi_G\rangle \tag{5}$$

which depends on the neutral ground state, its energy and the energy of the nth cation state, and the single-electron dipole matrix element between the neutral ground state and the scattered state.

We start with the simplest case of $N = 2$ where we can compute $a_n(\mathbf{k})$ and the ionization time delays, $\mathcal{T}_C$ and $\mathcal{T}_Q$, explicitly. The neutral molecule ground state can be expressed as a linear combination of the three noninteracting states $|\psi_n\rangle$, $|\Psi_G\rangle = \sum_{n=0}^{2} c_n|\Psi_n\rangle$, where the coefficients can be evaluated explicitly. In this case, we have two pathways corresponding to two states of the cation (ground and singly excited state). The corresponding amplitudes are obtained as $a_0(\mathbf{k}) = \mathcal{A}\mathrm{e}^{-1/4\alpha\left(E_{G0}+\omega_c-\frac{k^2}{2}\right)^2}(c_0\mathcal{B}(\mathbf{k}) + \mathrm{i}c_1 C(\mathbf{k}))$, with $\mathcal{A} = \frac{32\mathcal{E}}{\pi}\frac{q^{*7/2}k\sin(\vartheta)\mathrm{e}^{i\varphi}}{(q^{*2}+4k^2)^3}$ and

$$\mathcal{B}(\mathbf{k}) = \frac{24k\sin(2\vartheta)}{q^{*2}+4k^2}\cos\left(\frac{\mathbf{k}\cdot\hat{\mathbf{z}}R}{2}\right) + R\sin\left(\frac{\mathbf{k}\cdot\hat{\mathbf{z}}R}{2}\right)$$

$$C(\mathbf{k}) = \frac{24k\sin(2\vartheta)}{q^{*2}+4k^2}\sin\left(\frac{\mathbf{k}\cdot\hat{\mathbf{z}}R}{2}\right) - R\cos\left(\frac{\mathbf{k}\cdot\hat{\mathbf{z}}R}{2}\right) \tag{6}$$

where $E_{G0} = E_G - E_0$ is the energy difference between the neutral and cationic ground states and ϑ and φ denote polar angles for $\mathbf{k}$. Amplitude $a_1(\mathbf{k})$ is obtained from the expression for $a_0(\mathbf{k})$ by replacing c_0, c_1, and E_0 with c_1, c_2, and E_1, respectively. Note that the probability density $P(\mathbf{k})$ to ionize an electron in the range $\mathbf{k}$ and $\mathbf{k} + \mathrm{d}\mathbf{k}$ is $P(\mathbf{k}) = |a_0(\mathbf{k}) + a_1(\mathbf{k})|^2$ which vanishes as $\vartheta \to 0$. This is a reflection of the symmetry of the pi-electron density which has nodal plane containing the z-axis. Importantly, $P(\mathbf{k})$ also vanishes as $k \to 0$ and ∞.

https://doi.org/10.1021/acs.jpclett.4c00129
J. Phys. Chem. Lett. 2024, 15, 3866−3870

The ionization time delays[30] for the two pathways are then given by

$$\mathcal{T}_1(\mathbf{k}) = \frac{\hat{\mathbf{k}}\cdot\hat{\mathbf{z}}}{2k}\frac{c_0c_1R}{c_0^2\mathcal{B}^2(\mathbf{k}) + c_1^2C^2(\mathbf{k})}\left(R^2 + 96\frac{6k^2\sin^2(2\vartheta) + (q^{*2} - 4k^2)\sin(\vartheta)}{(q^{*2} + 4k^2)^2}\right) \quad (7)$$

$\mathcal{T}_2(\mathbf{k})$ is obtained by replacing $(c_0, c_1)\rightarrow (c_1, c_2)$ in eq 7. The interference contribution is

$$\mathcal{T}_Q(\mathbf{k}) = \frac{c_1^2 - c_0c_2}{2k}\frac{\mathcal{F}(\mathbf{k})}{\mathcal{D}(\mathbf{k})}\sin(\mathbf{k}\cdot\hat{\mathbf{z}}R) \times\left[\frac{\sin(\mathbf{k}\cdot\hat{\mathbf{z}}R)}{2}\mathcal{F}(\mathbf{k}) \frac{(c_1^4 - c_0^2c_1^2)(\mathcal{B}(\mathbf{k})C'(\mathbf{k}) - C(\mathbf{k})\mathcal{B}'(\mathbf{k}))}{(c_0^2\mathcal{B}^2(\mathbf{k}) + c_1^2C^2(\mathbf{k}))(c_1^2\mathcal{B}^2(\mathbf{k}) + c_2^2C^2(\mathbf{k}))} + \frac{k}{2\alpha}E_{10}\right] \quad (8)$$

where $\mathcal{F}(\mathbf{k}) = \left(\frac{24k\sin(2\vartheta)}{q^{*2} - 4k^2}\right)^2 - R^2 - \frac{48kR}{q^{*2} + 4k^2}\cot(\mathbf{k}\cdot\hat{\mathbf{z}}R)$ and $\mathcal{D}(\mathbf{k}) = (c_0e^{-\beta/2} + c_1e^{\beta/2})^2\mathcal{B}^2(\mathbf{k}) + (c_1e^{-\beta/2} + c_2e^{\beta/2})^2C^2(\mathbf{k})$ with $\beta = \frac{E_{10}}{2\alpha}\left(E_G + \omega_c - \frac{k^2}{2} - \frac{E_0}{2} - \frac{E_1}{2}\right)$.

As is evident from eqs 7 and 8, both $\mathcal{T}_C$ and $\mathcal{T}_Q$ diverge as $1/k$ near $k = 0$. However, this divergence is suppressed by the ionization probability $P(\mathbf{k})$ which vanishes more rapidly as k^2 near $k \rightarrow 0$.

If the ground state $|\Psi_G\rangle$ is given by a single Slater determinant, that is, when the electron−electron correlations are ignored, $c_1 = c_2 = 0$ and both $\mathcal{T}_1$ and $\mathcal{T}_2$ vanish, and hence the time delay $\mathcal{T}_C = 0$. This is valid for all values of N, indicating that $\mathcal{T}_C$ contribution vanishes for any noninteracting system.

In this particular case with $N = 2$, the time delay $\mathcal{T}_Q$ also vanishes since, in the absence of electronic correlation, there is only one pathway corresponding to the ground cationic state and hence there is no interference contribution. Special preparation of the initial state of the neutral molecule allows us to control both of the contributions. If the initial state is such that $c_1 = 0$, the interference time delay is nonzero while the other contribution vanishes. Similarly, if $c_1 = \sqrt{c_0c_2}$, the interference contribution vanishes. It is worth noting that although the ionization probability is maximum along $\vartheta = \pi/2$, *i.e.*, perpendicular to the molecular axis, both contributions to the time delay vanish. Hence the net ionization time delay vanishes along $\vartheta = \pi/2$. However, this vanishing time delay along $\vartheta = \pi/2$ is due to the zero phase of the electron wavepacket; and not due to the zero derivative of the phase; therefore it does not indicate an instantaneous ionization time delay along $\vartheta = \pi/2$.

The ionization time is independent of the pulse amplitude but depends on the time-scale of the pulse through the parameter α. For a spectrally narrow pulse $\alpha \rightarrow 0$, the time delay $\mathcal{T}_Q(\mathbf{k}) \rightarrow 0$, unless the pulse (central) frequency (ω_c) is such that $\omega_c - k^2/2 = (E_0 + E_1)/2 - E_G$, when $\mathcal{T}_Q(\mathbf{k}) \rightarrow \infty$, while the phase of the electron wavepacket, ϕ, is independent of α. The time delay $\mathcal{T}_C$, on the other hand, remains finite and nonzero in this limit. Thus, the pulse shape (in this case the width) allows control of the interference contribution to the time delay. The variations in $\mathcal{T}_C$ and $\mathcal{T}_Q$ with the ionized electron momentum k are displayed in Figure 1 for various values of the pulse width. Although both contributions show nonmonotonic variations with k, $\mathcal{T}_C$ shows a regular increase with α while $\mathcal{T}_Q$ shows more irregular variations, typical of an interference. Interestingly, in the entire parameter range explored in this work, the $\mathcal{T}_C$ is always positive while $\mathcal{T}_Q$ takes both positive and negative values.

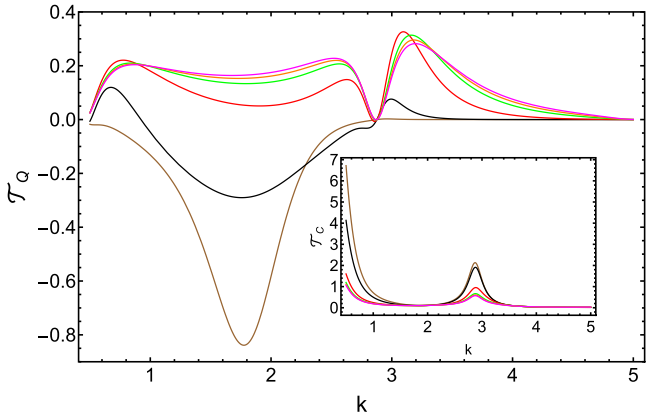

Figure 1. Interference time delay as a function of the ionized electron momentum k along $\theta = \pi/4$, $\phi = 0$ for the pulse width $\alpha = 0.05$, 0.10, 0.30, 0.60, 0.80, 1.00 (bottom to top at $k = 1.8$) and $\omega_c = 2.5$ *au*. Inset shows variation in $\mathcal{T}_C(\mathbf{k})$. Values of the other parameters are $R = 2.4$ au, $q = 1$, $c_0 = 0.894$, $c_1 = 0.1$, and $c_2 = 0.43$.

As the pulse bandwidth $(\propto\alpha)$ is decreased, the energy of the ionizing radiation field becomes well-defined at ω_c, and in the extreme case of $\alpha \rightarrow 0$, the pulse spectrum is a delta-pulse containing energy ω_c. In this case, only one pathway, let us say the nth pathway belonging to nth state of the cation that satisfies energy conservation $\omega_c - k^2/2 = E_n - E_G$, contributes to the ionization, and therefore, there is no interference contribution. As a result, the interference contribution decreases as the pulse spectral-width is decreased. Another parameter that effects the number of pathways within a fixed bandwidth of the pulse is the number of carbon atoms or conjugation in the molecule. As the conjugation is increased, the electron delocalization increases which results in smaller energy differences between different cationic states, thus leading to larger number of pathways. We thus expect that the interference contribution should increase as the conjugation in increased, as observed in a recent experiment on water clusters. Although increasing conjugation also affects $\mathcal{T}_C$ through probability $\mathcal{P}$, we find that the interference contribution dominates and is mainly responsible for the observed increase in the ionization time delay with the conjugation. Figure 2 depicts variations in both components as the conjugation is increased for three different values of the pulse width. It is evident that $\mathcal{T}_C$ is relatively insensitive to the pulse spectral width while $\mathcal{T}_Q$ decreases with the spectral width.

In conclusion, the total ionization time delay in molecules has two contributions: (i) the time delay associated with different ionizing pathways that correspond to different cationic eigenstates and (ii) the time delay arising as a result of the interference between the pathways. The former contribution is relatively insensitive to the number of available

https://doi.org/10.1021/acs.jpclett.4c00129
J. Phys. Chem. Lett. 2024, 15, 3866−3870

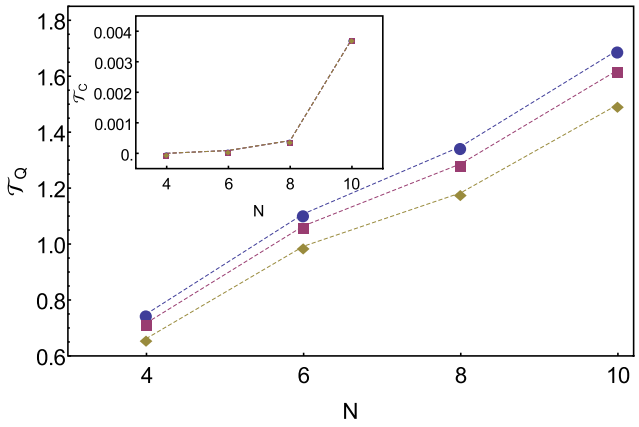

Figure 2. Interference contribution $\mathcal{T}_Q$ to the net time delay averaged over **k** with increasing conjugation for two ionizing pulses with spectral widths α = 0.25, 0.30, 0.35 (from bottom to top). Inset: Contribution from $\mathcal{T}_C$ remains small and depends weakly on the conjugation and the pulse width.

pathways and the conjugation in the molecule while the latter shows significant dependence and can be controlled by manipulating the ionizing pulse shape. The observed increase in the ionization time delay with conjugation seems to be originating entirely due to the interference contribution. Specific preparations of the initial molecular states and experimental schemes can allow us to measure the two contributions independently.

■ ASSOCIATED CONTENT

Supporting Information

The Supporting Information is available free of charge at https://pubs.acs.org/doi/10.1021/acs.jpclett.4c00129.

Derivation of eq 5 from Schrödinger's Equation; calculation of time delay $\mathcal{T}_C$ and $\mathcal{T}_Q$ in eq 3; calculation of $\mathcal{T}_C$ and $\mathcal{T}_Q$ for a diatomic molecule; and quantum chemistry calculation for ionization time delay (PDF)

■ AUTHOR INFORMATION

Corresponding Authors

Deep Mukherjee − *Department of Inorganic and Physical Chemistry, Indian Institute of Science, Bangalore 560012, India;* orcid.org/0000-0002-2979-5092; Email: deepm@iisc.ac.in

Upendra Harbola − *Department of Inorganic and Physical Chemistry, Indian Institute of Science, Bangalore 560012, India;* orcid.org/0000-0003-4053-8641; Email: uharbola@iiisc.ac.in

Author

Shaul Mukamel − *Department of Chemistry, University of California, Irvine, California 92697, United States;* orcid.org/0000-0002-6015-3135

Complete contact information is available at: https://pubs.acs.org/10.1021/acs.jpclett.4c00129

Notes

The authors declare no competing financial interest.

■ ACKNOWLEDGMENTS

D.M. acknowledges Department of Inorganic and Physical Chemistry, Indian Institute of Science, India, for computational facilities. U.H. acknowledges support from Science and Engineering Board (SERB), India, through the Grant No. CRG/2020/0011100. S.M. gratefully acknowledges the support of the National Science Foundation through Grant No. CHE- 2246379.

■ REFERENCES

(1) Weinkauf, R.; Schanen, P.; Yang, D.; Soukara, S.; Schlag, E. W. Elementary processes in peptides: electron mobility and dissociation in peptide cations in the gas phase. *J. Phys. Chem.* **1995**, *99* (28), 11255−11265.

(2) Remacle, F.; Levine, R. D. An electronic time scale in chemistry. *Proc. Natl. Acad. Sci. U. S. A.* **2006**, *103* (18), 6793−6798.

(3) Gruson, V.; Barreau, L.; Jiménez-Galan, A.; Risoud, F.; Caillat, J.; Maquet, A.; et al. Attosecond dynamics through a Fano resonance: Monitoring the birth of a photoelectron. *Science* **2016**, *354* (6313), 734−738.

(4) Isinger, M.; Squibb, R. J.; Busto, D.; Zhong, S.; Harth, A.; Kroon, D.; et al. Photoionization in the time and frequency domain. *Science* **2017**, *358* (6365), 893−896.

(5) Ossiander, M.; Siegrist, F.; Shirvanyan, V.; Pazourek, R.; Sommer, A.; Latka, T.; et al. Attosecond correlation dynamics. *Nat. Phys.* **2017**, *13* (3), 280−285.

(6) Peschel, J.; Busto, D.; Plach, M.; Bertolino, M.; Hoflund, M.; Maclot, S.; et al. Attosecond dynamics of multi-channel single photon ionization. *Nat. Commun.* **2022**, *13* (1), 5205.

(7) Hentschel, M.; Kienberger, R.; Spielmann, C.; Reider, G. A.; Milosevic, N.; Brabec, T.; et al. Attosecond metrology. *Nature* **2001**, *414* (6863), 509−513.

(8) Krausz, F.; Ivanov, M. Attosecond physics. *Rev. Mod. Phys.* **2009**, *81* (1), 163.

(9) Kienberger, R.; Goulielmakis, E.; Uiberacker, M.; Baltuska, A.; Yakovlev, V.; Bammer, F.; et al. Atomic transient recorder. *Nature* **2004**, *427* (6977), 817−821.

(10) Sansone, G.; Poletto, L.; Nisoli, M. High-energy attosecond light sources. *Nat. Photonics* **2011**, *5* (11), 655−663.

(11) Gaumnitz, T.; Jain, A.; Pertot, Y.; Huppert, M.; Jordan, I.; Ardana-Lamas, F.; Wörner, H. J. Streaking of 43-attosecond soft-X-ray pulses generated by a passively CEP-stable mid-infrared driver. *Opt. Express* **2017**, *25* (22), 27506−27518.

(12) Drescher, M.; Hentschel, M.; Kienberger, R.; Uiberacker, M.; Yakovlev, V.; Scrinzi, A.; et al. Time-resolved atomic inner-shell spectroscopy. *Nature* **2002**, *419* (6909), 803−807.

(13) Sansone, G.; Kelkensberg, F.; Pérez-Torres, J. F.; Morales, F.; Kling, M. F.; Siu, W.; et al. Electron localization following attosecond molecular photoionization. *Nature* **2010**, *465* (7299), 763−766.

(14) Belshaw, L.; Calegari, F.; Duffy, M. J.; Trabattoni, A.; Poletto, L.; Nisoli, M.; Greenwood, J. B. Observation of ultrafast charge migration in an amino acid. *J. Chem. Phys. Lett.* **2012**, *3* (24), 3751−3754.

(15) Lépine, F.; Ivanov, M. Y.; Vrakking, M. J. Attosecond molecular dynamics: fact or fiction? *Nat. Photonics* **2014**, *8* (3), 195−204.

(16) Calegari, F.; Ayuso, D.; Trabattoni, A.; Belshaw, L.; De Camillis, S.; Anumula, S.; et al. Ultrafast electron dynamics in phenylalanine initiated by attosecond pulses. *Science* **2014**, *346* (6207), 336−339.

(17) Nisoli, M.; Decleva, P.; Calegari, F.; Palacios, A.; Martín, F. Attosecond electron dynamics in molecules. *Chem. Rev.* **2017**, *117* (16), 10760−10825.

(18) Pazourek, R.; Nagele, S.; Burgdörfer, J. Attosecond chronoscopy of photoemission. *Rev. Mod. Phys.* **2015**, *87* (3), 765.

(19) Cavalieri, A. L.; Müller, N.; Uphues, T.; Yakovlev, V. S.; Baltuška, A.; Horvath, B.; et al. Attosecond spectroscopy in condensed matter. *Nature* **2007**, *449* (7165), 1029−1032.

(20) Schultze, M.; Fieß, M.; Karpowicz, N.; Gagnon, J.; Korbman, M.; Hofstetter, M.; et al. Delay in photoemission. *science* **2010**, *328* (5986), 1658−1662.
(21) Huppert, M.; Jordan, I.; Baykusheva, D.; Von Conta, A.; Wörner, H. J. Attosecond delays in molecular photoionization. *Phys. Rev. Lett.* **2016**, *117* (9), 093001.
(22) Sainadh, U. S.; Xu, H.; Wang, X.; Atia-Tul-Noor, A.; Wallace, W. C.; Douguet, N.; et al. Attosecond angular streaking and tunnelling time in atomic hydrogen. *Nature* **2019**, *568* (7750), 75−77.
(23) Gong, X.; Heck, S.; Jelovina, D.; Perry, C.; Zinchenko, K.; Lucchese, R.; Wörner, H. J. Attosecond spectroscopy of size-resolved water clusters. *Nature* **2022**, *609* (7927), 507−511.
(24) Muller, H. G. Reconstruction of attosecond harmonic beating by interference of two-photon transitions. *Appl. Phys. B: Laser Opt.* **2002**, *74*, s17−s21.
(25) Cattaneo, L.; Vos, J.; Lucchini, M.; Gallmann, L.; Cirelli, C.; Keller, U. Comparison of attosecond streaking and RABBITT. *Opt. Express* **2016**, *24* (25), 29060−29076.
(26) Mukherjee, D.; Harbola, U. Photo-Ionization Time Delay in Linearly Extended p-Conjugated Molecular Systems. *J. Phys. Chem. A* **2021**, *125* (38), 8417−8425.
(27) Heck, S.; Han, M.; Jelovina, D.; Ji, J. B.; Perry, C.; Gong, X.; et al. Two-Center Interference in the Photoionization Delays of Kr_2. *Phys. Rev. Lett.* **2022**, *129* (13), 133002.
(28) Wigner, E. P. Lower limit for the energy derivative of the scattering phase shift. *Phys. Rev.* **1955**, *98* (1), 145.
(29) Ivanov, M. Y.; Spanner, M.; Smirnova, O. Anatomy of strong field ionization. *J. Mod. Opt.* **2005**, *52* (2−3), 165−184.
(30) See the Supporting Information.
(31) Scheunemann, D.; Järsvall, E.; Liu, J.; Beretta, D.; Fabiano, S.; Caironi, M. Charge transport in doped conjugated polymers for organic thermoelectrics. *Chem. Phys. Rev.* **2022**, *3*, 021309.
(32) Sutton, A. P. *Electronic structure of materials*; Clarendon Press: 1993.

https://doi.org/10.1021/acs.jpclett.4c00129
J. Phys. Chem. Lett. 2024, 15, 3866−3870